Sequential Importance Sampling Filtering for Target Tracking in Image Sequences

Marcelo G. S. Bruno, *Member, IEEE*

***Abstract*—We propose in this letter a new approach to direct target tracking in cluttered image sequences using sequential importance sampling (SIS). We use Gauss–Markov random field modeling to describe the clutter correlation and incorporate the clutter and target signature models into the design of the SIS tracking algorithm. We quantify the performance of the SIS tracker using a simulated image sequence generated from real infrared airborne radar data and compare it to the performance of a grid-based hidden Markov model tracker. Simulation results show good performance for the proposed algorithms in a scenario of very low target-to-clutter ratio.**

***Index Terms*—Bayesian estimation, Gauss–Markov random fields (GMRF), particle filters, sequential importance sampling, target tracking.**

I. Introduction

We PRESENT in this letter new Bayesian algorithms for automatic tracking of cluttered targets in sequences of two-dimensional (2-D) digital images. Most conventional approaches to target tracking from images [1], [2] are based on the suboptimal association of a single frame image correlation filter and a linear Kalman–Bucy tracking filter (KBf). Such association has been shown [3] to perform poorly in scenarios of heavily cluttered targets. To overcome this limitation, we propose instead a Bayesian methodology that allows for direct target tracking from the image sequence and fully incorporates the models for target motion, target signature, and background clutter correlation.

We introduced in [3] a recursive point-mass hidden Markov model (HMM) filter for Bayesian tracking in image sequences. The point-mass filter in [3] was shown to outperform the correlation filter/KBf association, but it had the disadvantage of being computationally intensive. Here, we adopt a different strategy using a continuous-valued target state vector and sequential importance sampling (SIS) [6], [7], also known as particle filtering. We propose two different SIS trackers, based respectively on the sampling/importance resampling (SIR) or bootstrap filter [6], [7] and on the auxiliary particle filter (APF) [8].

We adapt the SIS filters to the problem of direct tracking from images by introducing a likelihood function that incorporates the target signature and clutter models. To describe the spatial correlation of the clutter, we use a 2-D noncausal Gauss–Markov random field (GMRf) model [9]. The parameters of the GMrf clutter model are estimated from the image sequence using an approximate maximum-likelihood (AML) estimator [9], [10]. In Sections II–V, we detail the proposed SIS trackers and discuss their performance.

Manuscript received March 8, 2002; revised October 14, 2002. The associate editor coordinating the review of this manuscript and approving it for publication was Prof. Visa Koivunen.

The author is with Instituto Tecnológico de Aeronáutica, São José dos Campos SP 12228-900, Brazil (e-mail: bruno@ele.ita.br).

Digital Object Identifier 10.1109/LSP.2003.814396

II. Target Motion Model

We denote the two dimensions of the plane, respectively, by the indexes $i = 1$ and $i = 2$. Let $\mathbf{x}_{n,i}$, $i = 1, 2$, be a vector that contains the position and velocity of the target centroid in dimension i at instant $t = n\Delta$, where n is an integer number, and Δ is the sampling period in time. The unknown target state vector is defined as

$$\mathbf{x}_n = [\,\mathbf{x}_{n,1}^T \quad \mathbf{x}_{n,2}^T\,]^T. \tag{1}$$

We assume that the random sequences $\{\mathbf{x}_{n,1}\}$ and $\{\mathbf{x}_{n,2}\}$ are statistically independent and that the centroid position and velocity in each dimension evolve in time according to the white-noise acceleration model [1]

$$\mathbf{x}_{n+1,i} = \underbrace{\begin{bmatrix} 1 & \Delta \\ 0 & 1 \end{bmatrix}}_{\mathbf{F}} \mathbf{x}_{n,i} + \mathbf{u}_{n,i}, \qquad n \geq 0,\ i = 1, 2 \tag{2}$$

where $\mathbf{u}_{n,i}$ is a zero-mean Gaussian vector such that

$$E\left[\mathbf{u}_{n,i}\mathbf{u}_{l,j}^T\right] = \underbrace{q\begin{bmatrix} \frac{\Delta^3}{3} & \frac{\Delta^2}{2} \\ \frac{\Delta^2}{2} & \Delta \end{bmatrix}}_{\mathbf{Q}} \delta_{n-l,i-j}. \tag{3}$$

In (3), $E[.]$ denotes expected value or ensemble average; q is a positive real number that is assumed known; and $\delta_{r,s}$ is the 2-D unit sample sequence such that $\delta_{r,s} = 1$ if $(r, s) = (0, 0)$ and zero otherwise.

III. Observation and Clutter Model

A remote sensing device generates raw measurements of a surveillance region that contains both targets of interest and undesired reflectors (clutter). For simplicity, we assume that there is only one single target of interest present at the scene at each sensor scan. The raw sensor measurements are sampled and processed to form a sequence of 2-D digital images, referred to as *frames*. Frame n is modeled by the $L \times M$ matrix

$$\mathbf{Y}_n = \mathbf{H}\left(\mathbf{x}_n^*\right) + \mathbf{V}_n \tag{4}$$

where matrix $\mathbf{V}_n$ represents the background clutter, and matrix $\mathbf{H}(\mathbf{x}_n^*)$ is the clutter-free target image, which is a function of the 2-D pixel location of the target centroid $\mathbf{x}_n^*$. The 2×1 hidden vector $\mathbf{x}_n^*$ is defined on the finite grid $\mathcal{L} = \{(i, j) \mid 1 \leq i \leq$

L, $1 \leq j \leq M\}$ and is obtained from the continuous-valued state vector $\mathbf{x}_n$ in (1) by making

$$x_n^*(1) = \text{round}\left(\frac{x_{n,1}(1)}{\Delta_x}\right) \quad (5)$$

$$x_n^*(2) = \text{round}\left(\frac{x_{n,2}(1)}{\Delta_y}\right) \quad (6)$$

where Δ_x and Δ_y are the image resolutions, respectively, in dimensions $i = 1$ and $i = 2$.

Target Model: We assume that, in any given frame, the clutter-free target image is contained in a bounded rectangular region of size $(r_i + r_s + 1) \times (l_i + l_s + 1)$. In this notation, r_i and r_s denote the maximum vertical pixel distances in the target image when we move away, respectively up and down, from the target centroid. Analogously, l_i and l_s are the maximum horizontal pixel distances in the target image when we move away, respectively left and right, from the target centroid. For each pixel centroid position $(i, j) \in \mathcal{L}$, the nonlinear function $\mathbf{H}$ in (4) returns a spatial distribution of (real-valued) pixel intensities $\{a_{k,l}\}$, $-r_i \leq k \leq r_s$, $-l_i \leq l \leq l_s$, centered at (i, j) (see [3] for details). For simplicity, the coefficients $\{a_{k,l}\}$, referred to as the target *signature parameters*, are assumed in this letter to be deterministic, known and frame-invariant.

Clutter Model: The clutter returns at frame n, $V_n(i, j)$, $1 \leq i \leq L$, $1 \leq j \leq M$, are described by the first-order, noncausal GMrf model [9]

$$V_n(i,j) = \beta_v^c \left[V_n(i-1,j) + V_n(i+1,j)\right] + \beta_h^c \left[V_n(i,j-1) + V_n(i,j+1)\right] + \varepsilon_n(i,j) \quad (7)$$

where the *unknown* parameters β_v^c and β_h^c are, respectively, the vertical and horizontal predictor coefficients, and ε_n is the prediction error such that $E[V_n(i,j)\varepsilon_n(l,r)] = \sigma_c^2 \delta_{i-l,j-r}$, with σ_c^2 also unknown. The assumption of zero-mean clutter implies a preprocessing of the data that subtracts the mean of the background. We also assume that, after preprocessing, the clutter frames $\{\mathbf{V}_n\}$ are statistically independent.

A. Likelihood Function

Let $\mathbf{y}_n$ be a one-dimensional long-vector representation of the frame $\mathbf{Y}_n$ obtained by row lexicographic ordering and use lowercase p to denote probability density functions (pdfs). Assuming a 2-D GMrf background as in (7) and deterministic signature parameters $\{a_{k,l}\}$, the likelihood function of the observed nth frame is [3]

$$p\left(\mathbf{y}_n \mid \mathbf{x}_{n,1}, \mathbf{x}_{n,2}\right) \propto \exp\left[\frac{2\lambda\left(\mathbf{x}_{n,1}, \mathbf{x}_{n,2}\right) - \rho}{2\sigma_c^2}\right] \quad (8)$$

where ρ is a target energy term that is constant away from the image borders (see [3] for details). The function λ in (8) is in turn given by

$$\lambda\left(\mathbf{x}_{n,1}, \mathbf{x}_{n,2}\right) = \sum_{k=-r_i}^{r_s} \sum_{l=-l_i}^{l_s} a_{k,l} \mu\left(x_n^*(1) + k, x_n^*(2) + l\right) \quad (9)$$

where $x_n^*(i), i = 1, 2$ are obtained, respectively, from (5) and (6), and $\mu(l, r)$ is the output of the differential filter

$$\mu(l,r) = Y_n(l,r) - \beta_h^c \left[Y_n(l,r-1) + Y_n(l,r+1)\right] - \beta_v^c \left[Y_n(l-1,r) + Y_n(l+1,r)\right] \quad (10)$$

TABLE I
ALGORITHM I: BOOTSTRAP FILTER FOR TARGET TRACKING IN 2-D CLUTTERED IMAGE SEQUENCES

1. Initialization For $j = 1, \ldots, N_p$
- Draw $\mathbf{x}_{0,1}^{(j)} \sim p(\mathbf{x}_{0,1})$, $\mathbf{x}_{0,2}^{(j)} \sim p(\mathbf{x}_{0,2})$,
make $w_0^{(j)} = 1/N_p$ and set $n = 1$.

2. Importance Sampling Step For $j = 1, \ldots, N_p$
- Draw $\tilde{\mathbf{x}}_{n,1}^{(j)} \sim N(\mathbf{F}\mathbf{x}_{n-1,1}^{(j)}, \mathbf{Q})$
and $\tilde{\mathbf{x}}_{n,2}^{(j)} \sim N(\mathbf{F}\mathbf{x}_{n-1,2}^{(j)}, \mathbf{Q})$.
- Compute the importance weights
$\tilde{w}_n^{(j)} \propto w_{n-1}^{(j)}\ p(\mathbf{y}_n \mid \tilde{\mathbf{x}}_{n,1}^{(j)}, \tilde{\mathbf{x}}_{n,2}^{(j)}) \qquad \sum_{j=1}^{N_p} \tilde{w}_n^{(j)} = 1$
using equations (8), (9), and (10).

3. Selection Step
- Generate a new set of samples
$\left\{\mathbf{x}_n^{(j)} = \left[(\mathbf{x}_{n,1}^{(j)})^T \ \ (\mathbf{x}_{n,2}^{(j)})^T\right]^T\right\} \qquad 1 \leq j \leq N_p$
such that $P(\left\{\mathbf{x}_n^{(j)} = \tilde{\mathbf{x}}_n^{(k)}\right\}) = \tilde{w}_n^{(k)}$.
- Make $w_n^{(j)} = 1/N_p$, $1 \leq j \leq N_p$.
- Set $n = n + 1$ and go back to step 2.

with Dirichlet (identically zero) boundary conditions. Equation (9) is valid for $r_i + 1 \leq x_n^*(1) \leq L - r_s$ and $l_i + 1 \leq x_n^*(2) \leq M - l_s$. For centroid positions near the image borders, the summation limits in (9) must be varied accordingly as explained in [3].

IV. Sequential Importance Sampling Tracker

Sequential importance sampling [4], [5] is a simulation approach to online Bayesian estimation where the posterior pdf of the hidden target state is represented at each instant n by a set of particles with associated importance weights. From the weighted particle set, we can then compute an estimate of the target state using, for example, a minimum mean-square error (MMSE) or a maximum *a posteriori* (MAP) criterion.

A. Bootstrap Tracker

The bootstrap filter [6] is a particular SIS algorithm that, at each instant n, draws a new set of particles from the Markovian transition kernel $p(\mathbf{x}_n \mid \mathbf{x}_{n-1})$, and updates the associated importance weights using the likelihood function $p(\mathbf{y}_n \mid \mathbf{x}_n)$. A selection step [4], [6], consisting of resampling from the particle set with replacement according to the importance weights, is added to prevent the distribution of particle weights from getting skewed as the number of iterations increase. Using the matrices $\mathbf{F}$ and $\mathbf{Q}$ introduced in (2) and (3) and recalling the likelihood function from Section III-A, we present in Table I a bootstrap filter algorithm for 2-D target tracking in image sequences.

B. Auxiliary Particle Filter Tracker

An SIS alternative to the bootstrap filter is the auxiliary particle filter [8]. The intuitive idea is to select a set of particles at instant n which, when propagated to instant $n + 1$, will have a high likelihood. This is formally accomplished by introducing an auxiliary index k, $1 \leq k \leq N_p$, and sampling at each instant n from the joint mixture importance function

$$\pi\left(k, \mathbf{x}_n \mid \mathbf{Y}_1^n\right) \propto p\left(\mathbf{y}_n \mid \underline{\mu}_n^{(k)}\right) p\left(\mathbf{x}_n \mid \mathbf{x}_{n-1}^{(k)}\right) \quad (11)$$

TABLE II
ALGORITHM II: MODIFIED IMPORTANCE SAMPLING STEP FOR APF TARGET TRACKING IN 2-D CLUTTERED IMAGE SEQUENCES

Importance Sampling Step For $j = 1, \ldots, N_p$

- Draw $\underline{\mu}_{n,1}^{(j)} \sim N(\mathbf{F}\mathbf{x}_{n-1,1}^{(j)}, \mathbf{Q})$ and $\underline{\mu}_{n,2}^{(j)} \sim N(\mathbf{F}\mathbf{x}_{n-1,2}^{(j)}, \mathbf{Q})$.
- Compute the first-stage importance weights $\lambda_n^{(j)} \propto p(\mathbf{y}_n \mid \underline{\mu}_{n,1}^{(j)}, \underline{\mu}_{n,2}^{(j)}) \qquad \sum_{j=1}^{N_p} \lambda_n(j) = 1$ using equations (8), (9), and (10).
- Draw $k^{(j)} \sim \{1, 2, \ldots, N_p\}$ with $\left\{P(\{k^{(j)} = i\}) = \lambda_n^{(i)}\right\}$, $i = 1, \ldots, N_p$.
- Draw $\tilde{\mathbf{x}}_{n,1}^{(j)} \sim N(\mathbf{F}\mathbf{x}_{n-1,1}^{(k^{(j)})}, \mathbf{Q})$ and $\tilde{\mathbf{x}}_{n,2}^{(j)} \sim N(\mathbf{F}\mathbf{x}_{n-1,2}^{(k^{(j)})}, \mathbf{Q})$.
- Compute the second-stage importance weights $\tilde{w}_n^{(j)} \propto w_{n-1}^{(k^{(j)})} \frac{p(\mathbf{y}_n \mid \tilde{\mathbf{x}}_{n,1}^{(j)}, \tilde{\mathbf{x}}_{n,2}^{(j)})}{p(\mathbf{y}_n \mid \underline{\mu}_{n,1}^{(k^{(j)})}, \underline{\mu}_{n,2}^{(k^{(j)})})} \qquad \sum_{j=1}^{N_p} \tilde{w}_n^{(j)} = 1$ using equations (8), (9), and (10).

where $\underline{\mu}_n^{(j)}$ is, for example, the mean of or a draw from $p(\mathbf{x}_n \mid \mathbf{x}_{n-1}^{(j)})$. Table II summarizes the modifications to the importance sampling step of the bootstrap tracker using auxiliary particles. The initialization and selection steps are identical to the same steps in Table I and are omitted accordingly.

C. Clutter Adaptation

We estimate the GMrf clutter parameters directly from each frame $\mathbf{Y}_n$ using the suboptimal *approximate maximum-likelihood* (AML) estimator introduced in [9]. The AML estimates $\widehat{\beta_h^c}$, $\widehat{\beta_v^c}$, and $\widehat{\sigma_c^2}$ at each frame are then plugged into (8) and (10) to compute $p(\mathbf{y}_n \mid \tilde{\mathbf{x}}_{n,1}^{(j)}, \tilde{\mathbf{x}}_{n,2}^{(j)})$. Table III summarizes the AML parameter estimation algorithm given the $L \times M$ frame $\mathbf{Y}_n$ (see [9] and [10] for further details).

V. PERFORMANCE RESULTS

We compare next the tracking performances of the bootstrap tracker, the APF tracker, and the HMM tracker using a simulated image sequence that is generated from real infrared airborne radar (IRAR) intensity imagery. The base image is a scene from the Portage IRAR database at Johns Hopkins University's Center for Imaging Sciences. We segmented the base image and estimated the spatially variant local means and the background clutter parameters. Each frame in the simulated image sequence is then generated by adding the local means to a different GMrf background sample synthetized with the estimated clutter parameters. Finally, we add to the background sequence a simulated target template that moves according to a white-noise acceleration model (see Section II), with parameters $q = 10$ and $\Delta = 4$ ms. The spatial resolution (pixel size) is $\Delta_x = \Delta_y = 20$ cm. The image frame extends from 0–30 m (150 pixels) in both the horizontal and vertical dimensions. The initial vertical and horizontal positions of the target are uniformly distributed, respectively, between 4–12 m and between 4–8 m. The initial vertical and horizontal target velocities are identically distributed Gaussian variables with mean 10 m/s and standard deviation 0.3162 m/s. Fig. 1(a) and (b) shows, respectively, the cluttered and clutter-free image of a target centered at pixel location (40,40). In the simulated cluttered image, the peak target-to-clutter ratio (PTCR) is 7.3 dB.

TABLE III
AML PARAMETER ESTIMATION ALGORITHM FOR AN $L \times M$ GMRF

a) Unnormalized sample correlations:
- $X_h = \sum_{i=1}^{L} \sum_{j=1}^{M-1} Y_n(i, j) Y_n(i, j+1)$.
- $X_v = \sum_{i=1}^{L-1} \sum_{j=1}^{M} Y_n(i, j) Y_n(i+1, j)$.

b) Unnormalized sample power:
- $S_y = \sum_{i=1}^{L} \sum_{j=1}^{M} Y_n^2(i, j)$.

c) Make $\delta = 10^{-3}$, compute $\epsilon = 0.5 - \delta$ and $\alpha = \frac{(L-1)M}{L(M-1)}$.

d) Correlation coefficients estimates:
- $\widehat{\beta_h^c} = \frac{\epsilon \chi_h}{|\chi_v|\cos(\frac{\pi}{L+1}) + \alpha|\chi_h|\cos(\frac{\pi}{M+1})}$.
- $\widehat{\beta_v^c} = \frac{\epsilon \chi_v}{|\chi_v|\cos(\frac{\pi}{L+1}) + \alpha|\chi_h|\cos(\frac{\pi}{M+1})}$.

e) Clutter power estimate:
- $\widehat{\sigma_c^2} = \frac{1}{LM}\left(S_y - 2\widehat{\beta_h^c} * X_h - 2\widehat{\beta_v^c} * X_v\right)$.

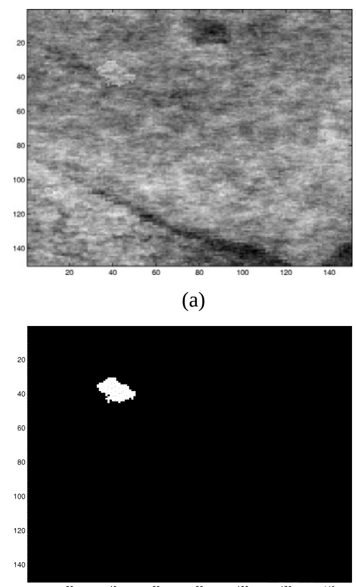

(a)

(b)

Fig. 1. (a) Simulated cluttered target image (PTCR= 7.3 dB). (b) Clutter-free target template shown as a binary image.

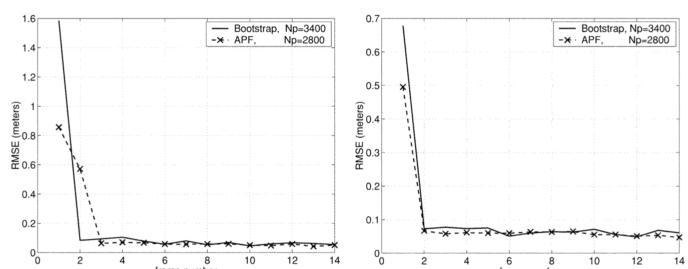

(a) (b)

Fig. 2. APF and bootstrap rmse in meters PTRC $= -5.7$ dB. (a) Vertical dimension. (b) Horizontal dimension.

Fig. 2(a) and (b) shows the rmse in meters of the MAP target centroid position estimates, respectively in the vertical and horizontal directions, obtained by a 3400-particle bootstrap (solid line) filter and by a 2800-particle APF (dashed line) with PTCR lowered to -5.7 dB. The SIS filters failed to converge to the true

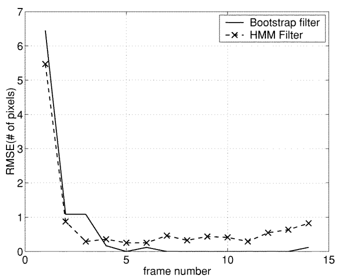

(a)

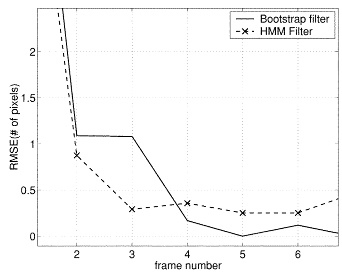

(b)

Fig. 3. RMSE in number of pixels for the bootstrap tracker (solid) and the HMM tracker (dashed), PTCR $= -5.7$ dB, vertical dimension. (a) Original scale. (b) Zoomed-in plot.

track in three out of 48 Monte Carlo runs. The error curves in Fig. 2(a) and (b) were obtained excluding the divergent tracks from the average. The plots show, that despite the low contrast between the target and the background, the particle filters quickly acquired the target after an initial error and tracked it with a low (less than 1 pixel) rmse. The reduction in the number of particles in the APF tracker seems not to have significantly affected steady-state performance.

For comparison purposes, we implemented a grid-based HMM tracker using a rough approximation of the continuous-valued motion model in Section II by a discrete-valued model consisting of a constant deterministic drift equal to two pixels/frame plus a first-order 2-D discrete random walk with probability of fluctuation of one pixel in both dimensions equal to 10%. Fig. 3(a) shows the rmse in number of pixels of the MAP vertical target position estimates generated by the bootstrap tracker (solid line) and the HMM filter (dashed line). Fig. 3(b) is a zoomed-in version of the same plot where the two curves can be seen more clearly. The bootstrap filter in this experiment failed to converge to the true track in three out of 50 Monte Carlo runs, while the HMM filter acquired the target in all Monte Carlo simulations. The error curves in Fig. 3(a) and (b) were obtained considering only the simulations in which both trackers converged. The plots show that, excluding the rare occasions when the bootstrap filter diverges, both the HMM and the SIS tracker have good tracking performance with a small target acquisition time. The slight deterioration in rmse for the HMM filter toward the final sequence frames may reflect the mismatch between the actual motion model and the approximate discrete-state model assumed by the grid-based tracker. The error curves for the horizontal position estimate are qualitatively similar and are omitted here for lack of space.

We close with a brief comment on computational complexity. The grid-based HMM filter from [3] requires the evaluation of the likelihood function in all points of the image grid. Assuming an $L \times L$ grid, such computation has cost $O(\alpha L^2)$, $\alpha \ll L$, in terms of required floating point multiplications. By contrast, the bootstrap particle filter requires the evaluation of the likelihood function for each particle $\tilde{\mathbf{x}}_n^{(j)}$ only, or a computational cost of order $O(\alpha N_p)$. The multinomial resampling routine in the selection step of the SIS filter is also implemented efficiently (see [4]) with computational cost $O(N_p)$. Overall, if $N_p \ll L^2$, the computational savings are considerable when we compare the HMM filter in [3] to the SIS trackers proposed in this letter.

VI. Conclusion

Conventional solutions to the problem of target tracking in image sequences based on the association of correlation filters and linear Kalman–Bucy filters are unreliable [3] in scenarios of very low target-to-clutter ratio. In this letter, we introduced alternative nonlinear Bayesian algorithms based on sequential importance sampling that enable direct tracking from the image sequence and fully incorporate the models for target motion, target signature, and background clutter.

We tested the performance of the proposed algorithms using simulated image sequences generated from real infrared airborne radar data. Monte Carlo simulation results show good tracking performance for the basic bootstrap tracker using 3400 particles in a scenario with a very dim target (PTCR $= -5.7$ dB). The steady-state rmse for a 2800-particle APF tracker was roughly identical to the steady-state rmse for the 3400-particle bootstrap filter suggesting that the additional algorithmic complexity of the APF is partly compensated by a possible reduction in the number of particles that are needed to achieve similar performance. Overall, the proposed SIS filters compared favorably to an alternative grid-based HMM tracker by yielding similar rmse performance at a much lower computational cost.

Acknowledgment

The author would like to thank the anonymous reviewers for their comments, which helped to improve this letter.

References

[1] Y. Bar-Shalom and X. Li, “Tracking with imaging sensors,” in *Multi-target-Multisensor Tracking: Principles and Techniques*. Storrs, CT: YBS, 1995.
[2] E. Oron, A. K. Kumar, and Y. Bar-Shalom, “Precision tracking with segmentation for imaging sensors,” *IEEE Trans. Aerosp. Electron. Syst.*, vol. 29, pp. 977–987, July 1993.
[3] M. G. S. Bruno and J. M. F. Moura, “Multiframe detection/tracking in clutter: Optimal performance,” *IEEE Trans. Aerosp. Electron. Syst.*, vol. 37, pp. 925–946, July 2001.
[4] M. S. Arulampalam, S. Maskell, N. Gordon, and T. Clapp, “A tutorial on particle filters for online nonlinear/non-Gaussian Bayesian tracking,” *IEEE Trans. Signal Processing*, vol. 50, pp. 174–188, Feb. 2002.
[5] A. Doucet, J. F. G. Freitas, and N. J. Gordon, “An introduction to sequential Monte Carlo methods,” in *Sequential Monte Carlo Methods in Practice*, A. Doucet, J. F. G. Freitas, and N. J. Gordon, Eds. New York: Springer-Verlag, 2001.
[6] N. J. Gordon, D. J. Salmond, and A. F. M. Smith, “Novel approach to nonlinear/non-Gaussian Bayesian state estimation,” *Proc. Inst. Elec. Eng. F*, vol. 140, no. 2, pp. 107–113, 1993.
[7] N. J. Gordon, D. J. Salmond, and C. Ewing, “Bayesian state estimation for tracking and guidance using the bootstrap filter,” *J. Guidance, Contr., Dynam.*, vol. 18, no. 6, pp. 1434–1443, 1995.
[8] M. K. Pitt and N. Shephard, “Filtering via simulation: Auxiliary particle filters,” *J. Amer. Stat. Assoc.*, vol. 94, no. 446, pp. 590–599, 1999.
[9] J. M. F. Moura and N. Balram, “Noncausal Gauss–Markov random fields: Parameter structure and estimation,” *IEEE Trans. Inform. Theory*, vol. 39, pp. 1333–1355, July 1993.
[10] S. M. Schweizer and J. M. F. Moura, “Hyperspectral imagery: Clutter adaptation in anomaly detection,” *IEEE Trans. Inform. Theory*, vol. 46, pp. 1855–1871, Aug. 2000.